

Supplementary Information

Tsc2-Rheb Signaling Regulates EphA-Mediated Axon Guidance

Du-yu Nie, Alessia Di Nardo, Juliette M. Han, Hasani Baharanyi, Ioannis Kramvis, ThanhThao Huynh, Sandra Dabora, Simone Codeluppi, Pier Paolo Pandolfi, Elena B. Pasquale, Mustafa Sahin

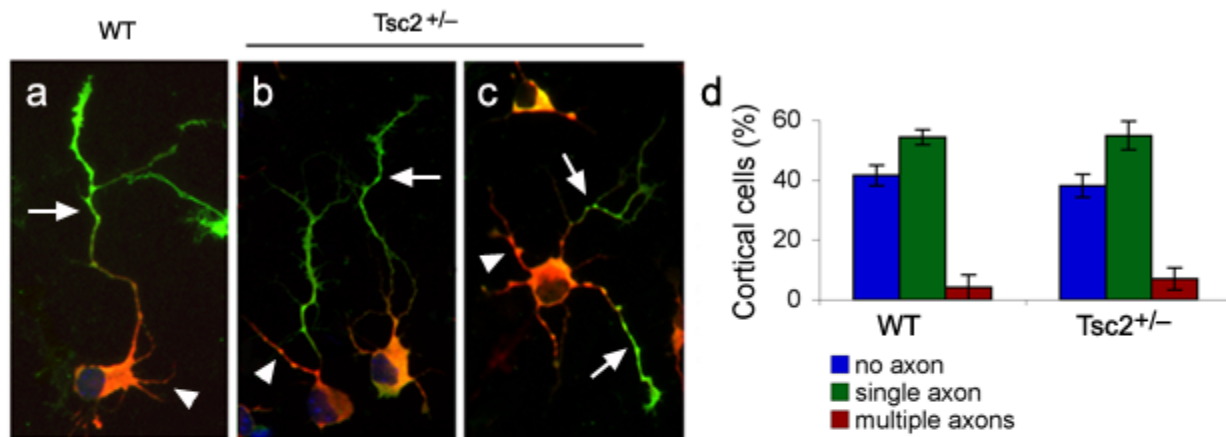


Figure S1. Normal polarity formation in *Tsc2*^{+/-} neurons.

E18 cortical neurons from wild-type (a) and *Tsc2*^{+/-} (b-c) littermates were stained with antibodies to an axon specific marker Tau1 (green) and somatodendrite marker MAP2 (red). (d) Quantification of the percentage of neurons with 0, 1 or multiple axons in *Tsc2*^{+/-} and wild-type cultures. Data represent mean ± s.e.m. (38.10 ± 3.87 % with no axons, 54.86 ± 4.75 % with single axon and 7.04 ± 3.72 % with multiple axons for *Tsc2*^{+/-} 41.55 ± 3.45 % with no axon, 54.29 ± 2.54 % with single axon and 4.17 ± 4.17 % with multiple axons for wild-types). No significant difference exists between wild-type and *Tsc2*^{+/-} (unpaired *t*-test).

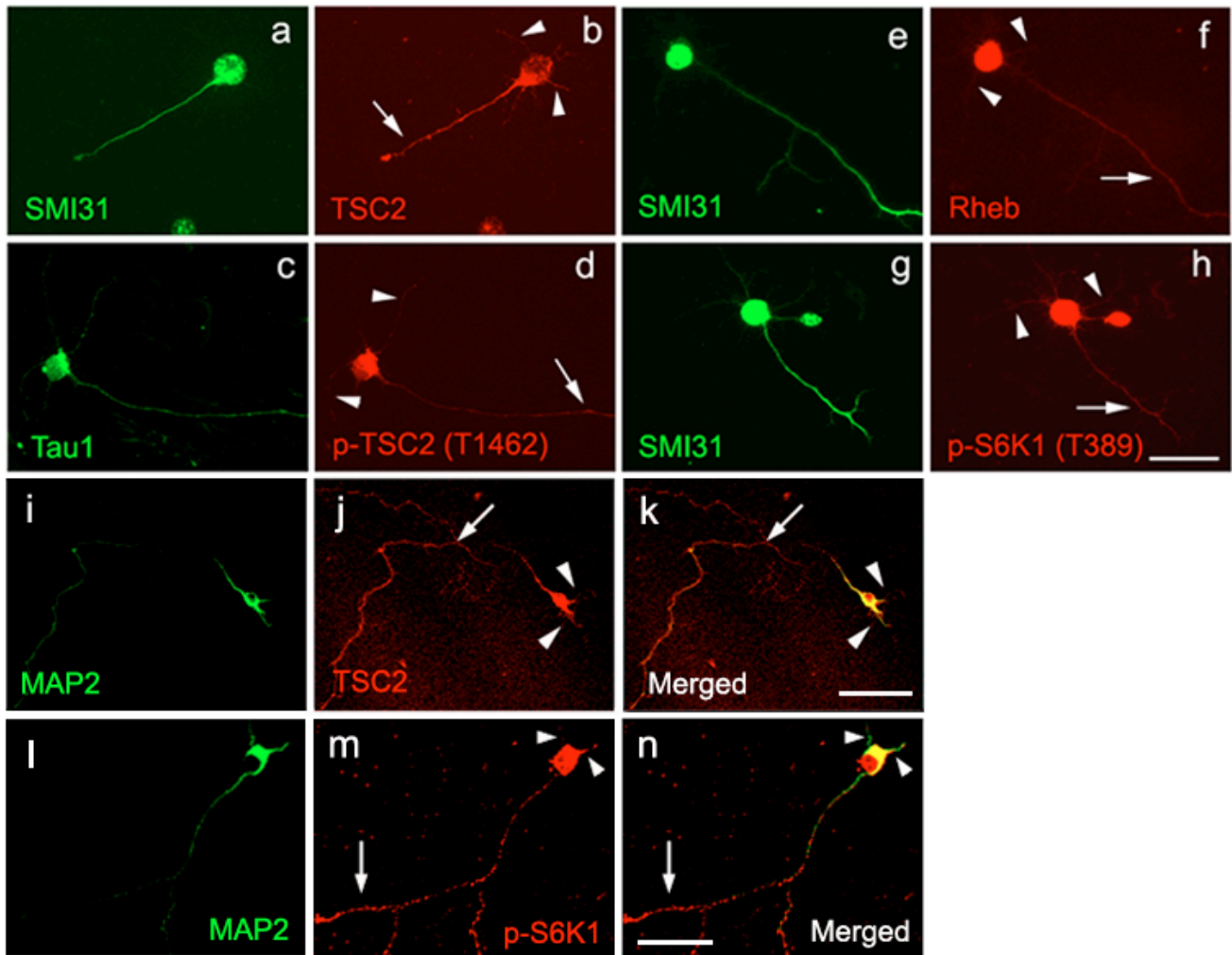


Figure S2. Subcellular expression of TSC-mTOR signaling components in purified RGCs.

RGCs purified from P8 rat pups were stained with antibodies to total TSC2 (red; b), phospho-TSC2 (Thr1462, red; d), Rheb (red; f), or phospho-S6K1 (Thr389, red; h) with an axonal marker SMI31 (green; a, e, g) or Tau1 (green, c). RGCs were also stained with antibodies to total TSC2 (red in g, k), phospho-S6K1 (Thr389, red in m, n) with the somatodendritic marker MAP2 (green in i, k, l and n). Scale bars, 100 μ m. Arrows and arrowheads denote axons and dendrites, respectively.

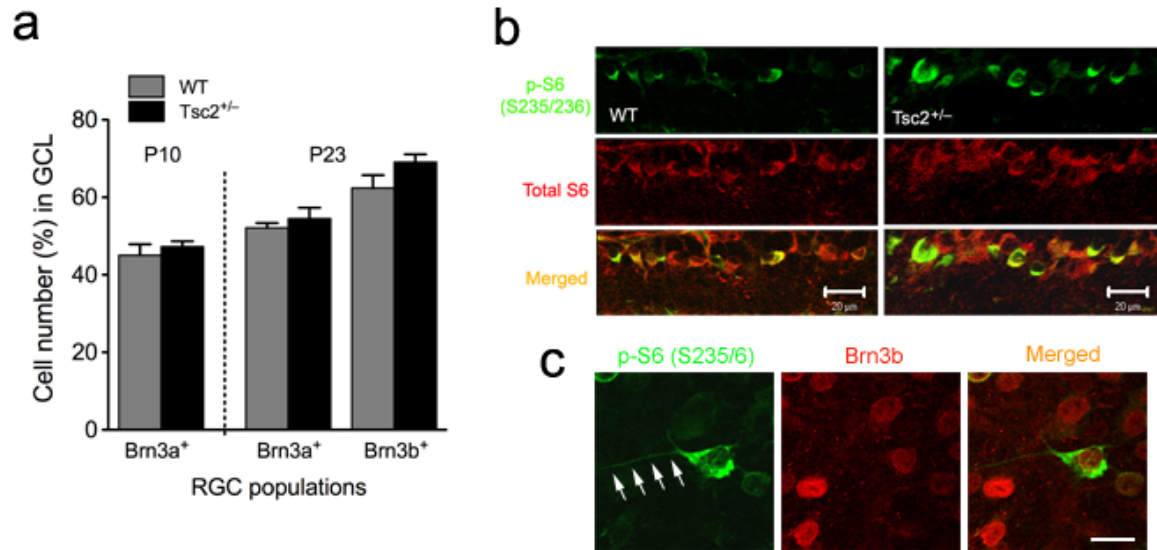


Figure S3. Number of Brn3⁺ RGCs and total S6 protein expression in the GCL of *Tsc2*^{+/-} retina do not differ from those in wild-type mice retina.

(a) Quantification of the percentage of Brn3a or Brn3b expressing cell in *Tsc2*^{+/-} versus wild-type retina ganglion cell layer (GCL). Total cell number in GCL is determined by Hoechst nuclei staining. Data are represented as mean \pm s.e.m. ($n = 5$ mice for each genotype). There is no significant difference in size of either Brn3a⁺ or Brn3b⁺ RGC populations between wild-type and *Tsc2*^{+/-} retina. (b) Horizontal retinal sections from *Tsc2*^{+/-} as well as wild-type littermates at P23 were stained with antibodies against total S6 (red) and phospho-S6 (Ser235/6) (green). Asterisks mark cells in yellow that are co-labeled with p-S6 and total S6. Scale bars, 20 μ m. (c) High power image showing co-labeling of phospho-S6 (S235/6, green) and Brn3b (red) as in Figure 1B. White arrows indicate phospho-S6 labeling of an RGC axon. Scale bars, 20 μ m.

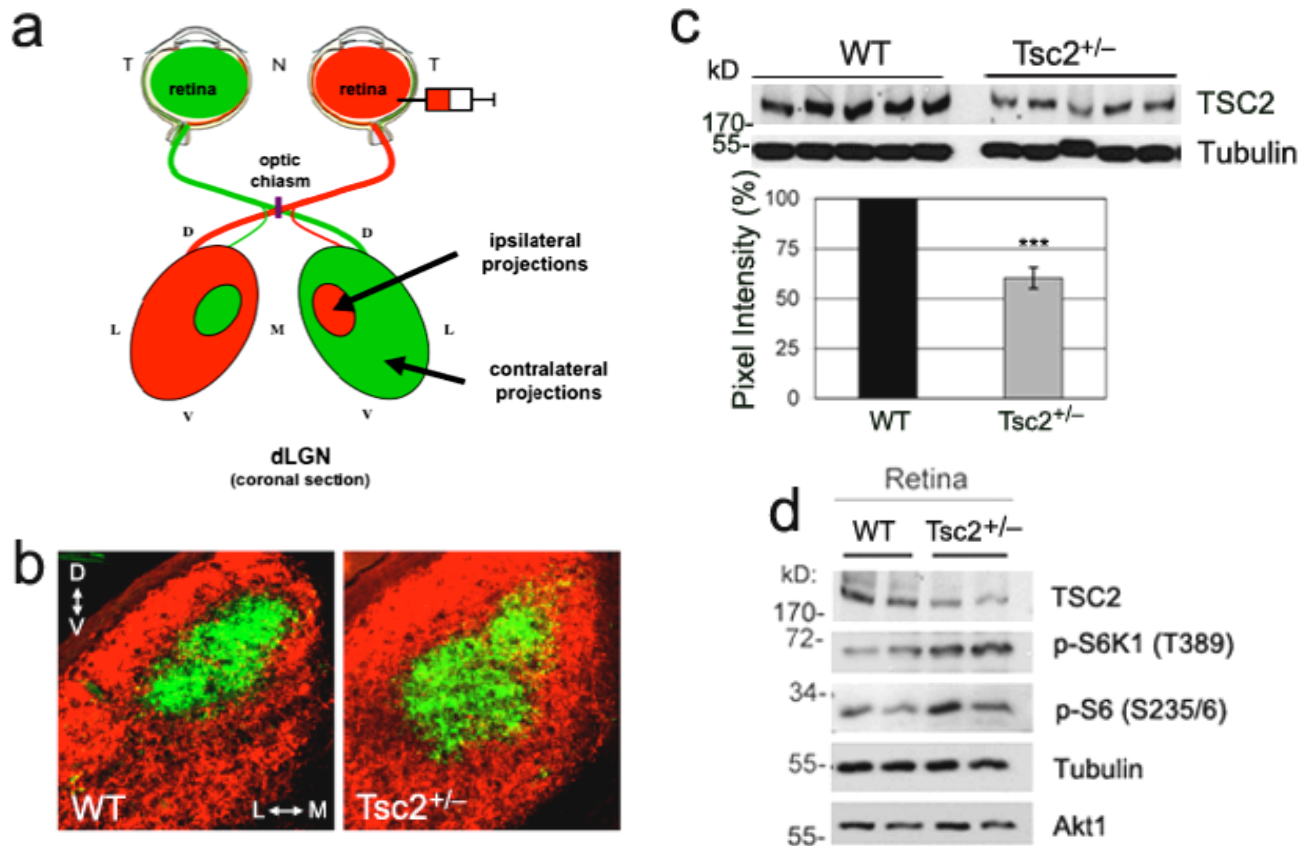


Figure S4. Analysis of axonal projections and mTOR activity in *Tsc2*^{+/-} mice.

(a) Schematic representation of the experimental strategy to label the retinogeniculate projections. Alexa594 (red) and Alexa488 (green) conjugated CTB are injected to left and right eye, respectively. The projections from both eyes in the dorsal lateral geniculate nuclei (dLGN) are differentiated by the fluorophores. (b) Representative images of labeled dLGN from P16 *Tsc2*^{+/-} and wild-type littermates (injected at P14). The ipsilateral projection (in green) appears more diffuse in *Tsc2*^{+/-} than wild-type littermates. N, nasal; T, temporal; D, dorsal; M, medial; L, lateral; V, ventral. (c) Cortical neurons isolated from *Tsc2*^{+/-} versus wild-type embryos (E18) were analyzed by westerns. The level of TSC2 protein in *Tsc2*^{+/-} neurons is 60.2 ± 11.6 % of that in wild-types. The error bar represents s.e.m. and *** P < 0.005 by t-test. (d) Western blotting analyses of retinal lysates of *Tsc2*^{+/-} versus wild-type littermates at P7. Tubulin and Akt1 are used as loading controls.

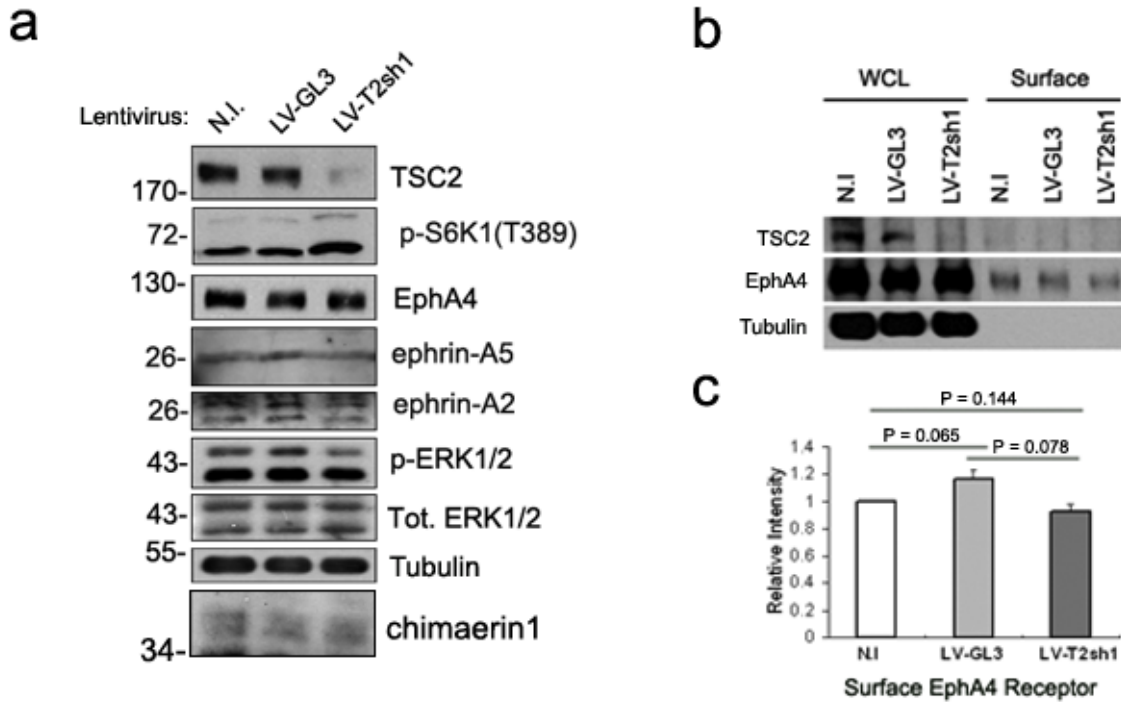


Figure S5. Tsc2 knockdown does not affect protein levels of EphA4, ephrins-A2/A5, chimaerin or ERK1/2.

(a) Cortical neurons were infected with lentiviruses expressing shRNA against a luciferase (GL3) or Tsc2 (T2sh1). The infected as well as non-infected neurons are analyzed in westerns for the proteins as indicated (tubulin used as a loading control). Tsc2 knockdown neurons show a slight decrease in phospho-ERK1/2 level and unchanged levels of EphA4, ephrinA2, ephrinA5 and chimaerin1, as compared to both controls. (b) GL3, T2sh1 lentivirus infected and non-infected (N.I) neurons were incubated with the membrane impermeable Sulfo-NHS-SS-Biotin (Pierce). Pull-downs of biotinylated cell surface proteins as well as whole cell lysates (WCL) were analyzed in westerns for the indicated proteins (tubulin as a loading control). (c) Quantification of EphA4 level in cell surface pull-down of infected versus non-infected neurons. Data are expressed as normalized to non-infected neurons and represent mean \pm s.e.m. from 3 independent experiments (1.162 ± 0.075 in GL3 and 0.922 ± 0.058 in T2sh1). EphA4 cell surface expression on Tsc2 knockdown neurons is not significantly affected (t-test).

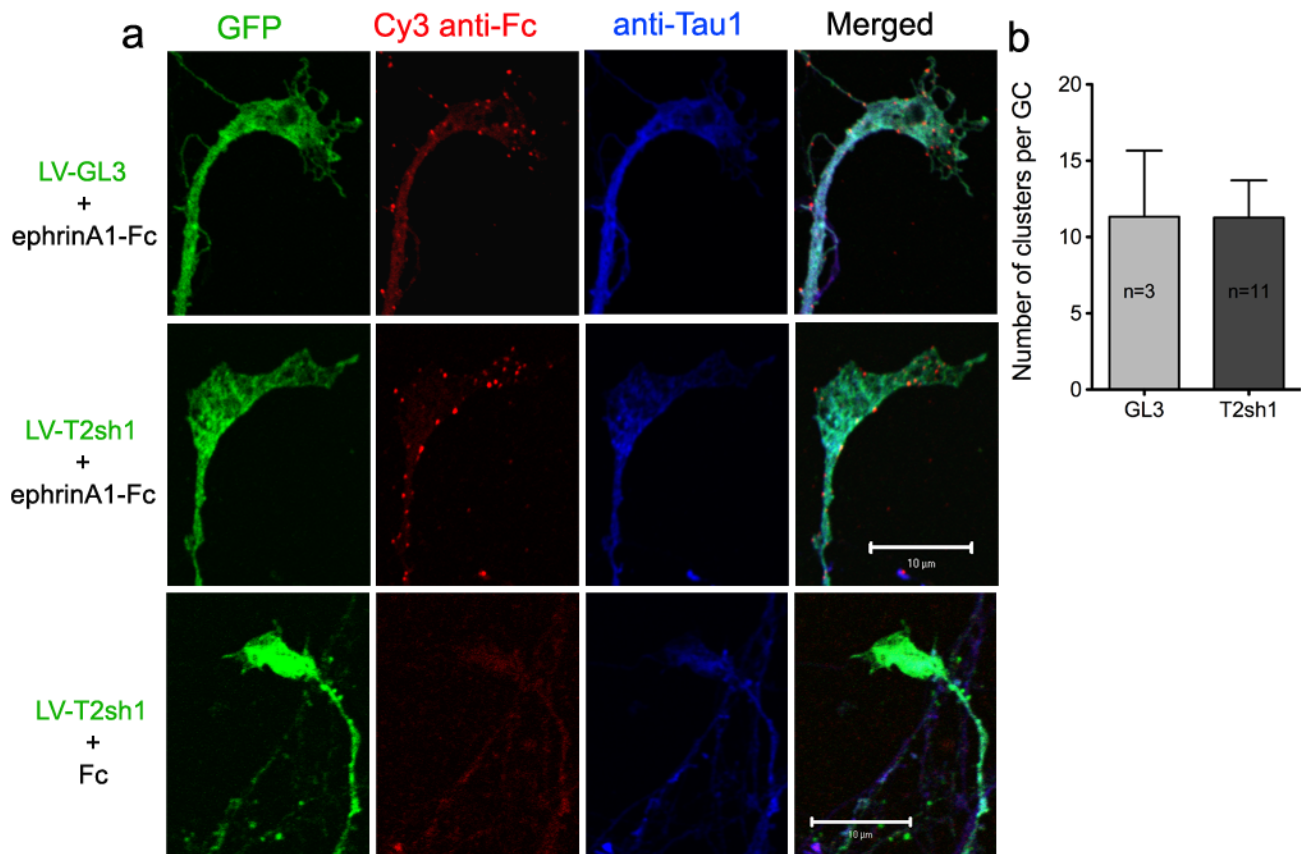


Figure S6. Ephrin-stimulated Eph receptor clustering appears normal in Tsc2 deficient neurons.

GL3 or T2sh1 infected neuronal cultures were stimulated with 1 $\mu\text{g/ml}$ pre-aggregated ephrin-A1-Fc or Fc for 5 minutes and then fixed for staining with Cy3-anti-human IgG Fc and anti-Tau1 (blue). **(a)** Representative confocal images showing EphA receptor clusters (red) in growth cones of GL3 or T2sh1 infected neurons (green). Fc stimulation does not induce EphA clusters while ephrin-stimulated clusters appear as puncta. Scale bars, 10 μm . **(b)** Quantification of cluster number per growth cone in T2sh1 versus GL3 infected neurons. Data represent mean \pm s.e.m. (GL3: 11.33 ± 4.33 , $n = 3$ growth cones; T2sh1: 11.27 ± 2.44 , $n = 11$ growth cones). No significant difference exists between control and T2sh1 infected neurons (t-test).

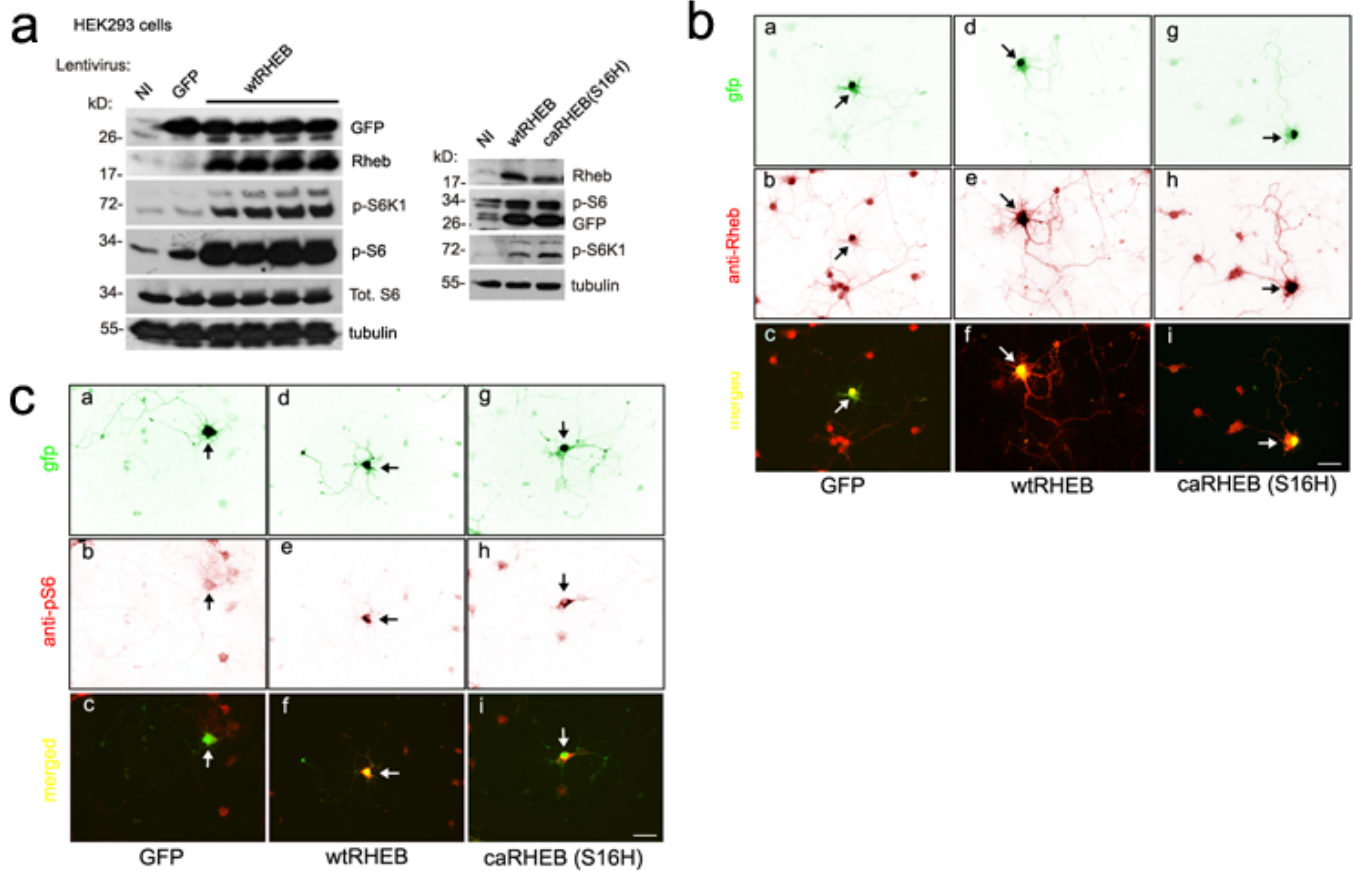


Figure S7. Lentiviral-based Rheb over-expression activates mTOR in HEK293 cells and neurons.

(a) HEK293 cells were infected with viruses encoding wild-type RHEB (wtRHEB), constitutively active RHEB mutant (caRHEB, S16H), GFP alone or left non-infected (NI). Western analyses verified over-expression of Rheb as well as robust activation of mTOR as shown by higher phospho-S6K1 (Thr389) and phospho-S6 (Ser235/6) levels in wtRHEB and caRHEB compared to GFP or non-infected neurons. Tubulin and total S6 are used as loading controls. (b) Hippocampal neurons infected with viruses expressing wtRHEB, caRHEB or GFP (green) were stained with anti-Rheb antibody (red). (c) Infected hippocampal neurons (green) were also stained with specific antibodies against phospho-S6 (Ser235/236) (red). Arrows depict infected neurons. Scale bars, 50 μ m.

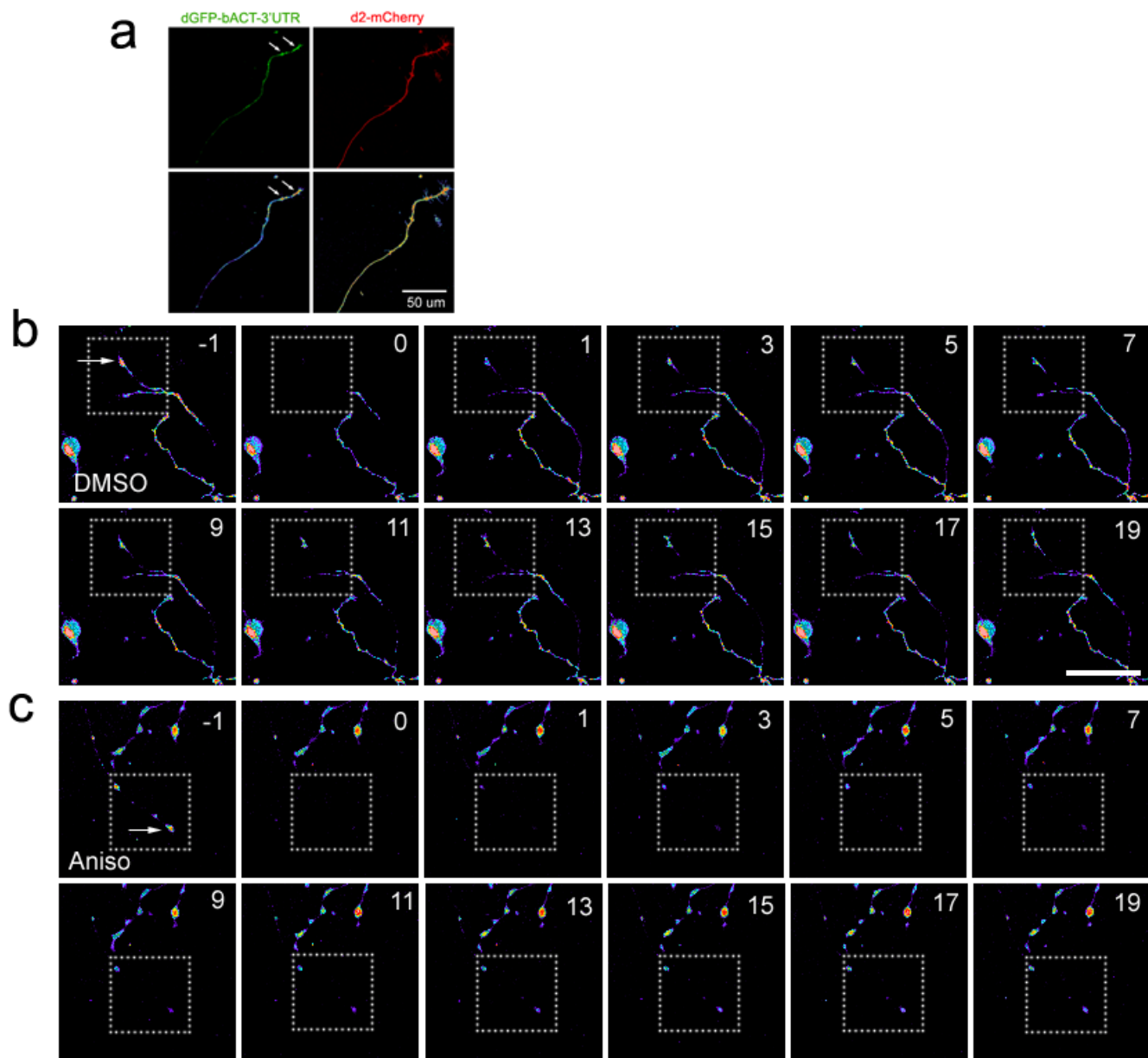


Figure S8. Fluorescence recovery after photobleaching analysis of the β -actin reporter in anisomycin treated axons.

(a) Representative images showing axons co-expressing dGFP^{myr}-bACT-3'UTR (green) and d2-mCherry (red). Differential signal intensity along the axon and growth cone is appreciable in converted spectrum displays. (b) Representative serial images showing GFP signal intensities at time points of pre-bleach and post-bleach over 20 min in a DMSO pre-treated axon. (c) Representative serial images showing GFP signal recovery over 20 min in an anisomycin pre-treated axon. Arrows indicate axonal growth cones. On each image, the number denotes minutes pre- or post-bleaching and dashed frame represents region of bleaching. Scale bars, 50 μ m.

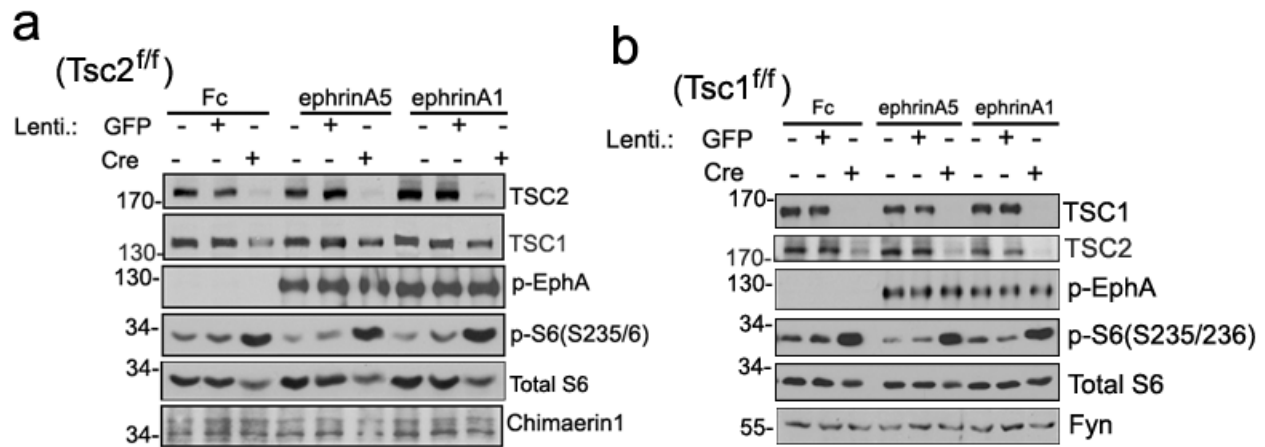


Figure S9. Loss of ephrin-induced decrease in S6 phosphorylation in *Tsc1* or *Tsc2* deficient mouse neurons.

Cortical neurons isolated from *Tsc2^{fllox/fllox}* (a) or *Tsc1^{fllox/fllox}* (b) embryos (E16.5) were infected with lentivirus expressing Cre recombinase, GFP or left non-infected. Western blot analyses were performed for indicated proteins with total S6 used as the loading control.

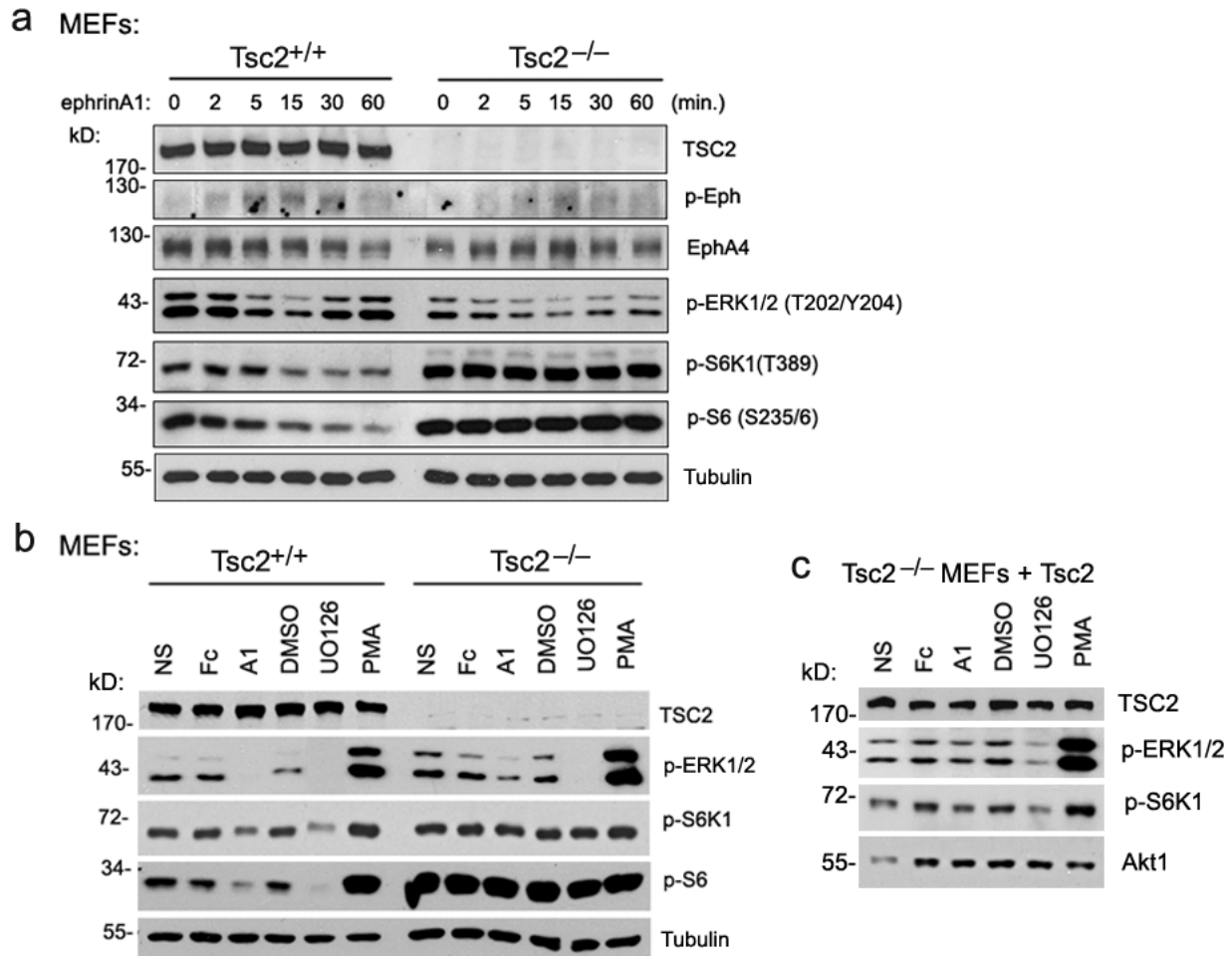


Figure S10. Regulation of mTOR activity by ephrin-A1 in *Tsc2*^{+/+} versus *Tsc2*^{-/-} MEFs.

(a) Time-course western analyses showing phosphorylation levels of EphA, ERK1/2, S6K1 and S6 in ephrin-A1 stimulations for *Tsc2*^{+/+} versus *Tsc2*^{-/-} mouse embryonic fibroblasts (MEFs). Note that total EphA4 is at comparable levels in *Tsc2*^{+/+} vs *Tsc2*^{-/-} MEFs. (b) Serum starved *Tsc2*^{+/+} and *Tsc2*^{-/-} MEFs are treated with indicated reagents (pre-aggregated ephrin-A1-Fc and Fc: 5 μ g/ml; UO126 and PMA: 25 μ M) for 30 minutes or left un-stimulated (NS). Western analyses of indicated proteins show that ephrin-A1 and UO126 inhibit phosphorylation of ERK1/2, S6K1 (Thr389) or S6 (Ser235/6) in *Tsc2*^{+/+}, but not in *Tsc2*^{-/-} MEFs. (c) Western analyses showing that retrovirus-based TSC2 reconstitution into *Tsc2*^{-/-} MEFs restores the effects of ephrin-A1 or UO126 treatment on ERK1/2 and S6K1 phosphorylation.

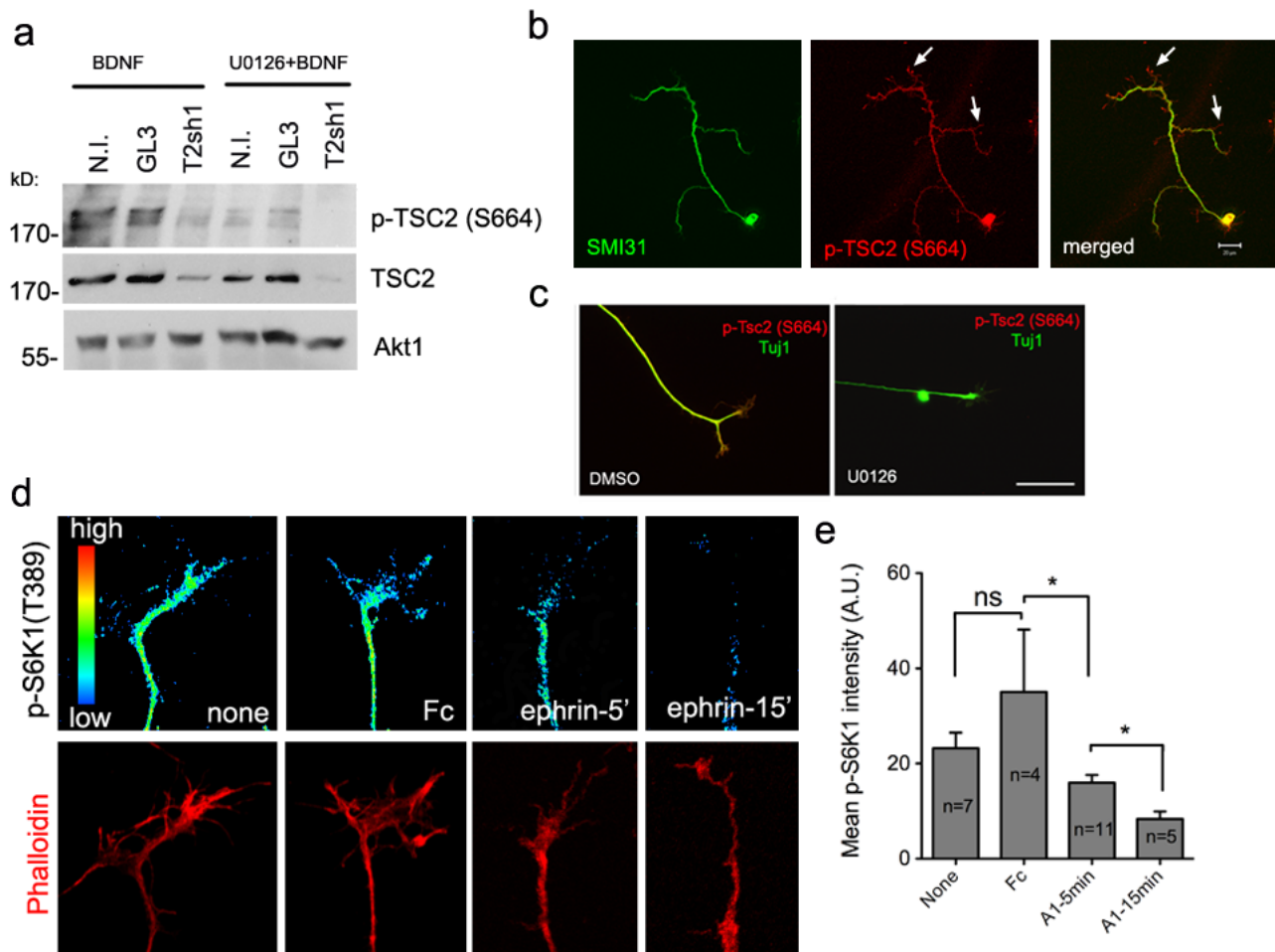


Figure S11. Reduction of phospho-TSC2 (Ser664) and phospho-S6K1 (T389) staining in ephrin stimulated RGC growth cones.

(a) GL3, T2sh1 infected or non-infected (N.I.) neurons were starved and stimulated with BDNF (50 ng/ml) alone or UO126 (50 μ M) followed by BDNF. Western analyses for phospho-TSC2 (S664) and total TSC2 were performed on the same blot, and Akt1 was used as the loading control. Phospho-TSC2 (Ser664) level is reduced upon UO126 treatment as well as in TSC2 knockdown cultures. (b) Purified RGC cultures were stained with anti-phospho-TSC2 (Ser664) and SMI31 as an axonal marker. Arrows indicate filopodia labeling by the phospho-TSC2 (Ser664). Scale bar, 20 μ m. (c) Representative images showing RGC growth cone staining with phospho-TSC2 (Ser664) (red) and Tuj1 (green), after treatment with U0126 (50 μ M) or DMSO for 30 minutes. Scale bar, 100 μ m. (d) Representative confocal images showing growth cone staining with anti-phospho-S6K1 (Thr389, green) and rhodamine-phalloidin (red) in RGC cultures under different stimulation conditions. Labeling of phospho-S6K1 (Thr389) was converted to pseudo-colored spectrum display. (e) Quantification of average phospho-S6K1 fluorescence intensity in RGC growth cones upon stimulations. Data represent mean \pm s.e.m. (non-stimulated: 23.20 \pm 3.26, n = 7 growth cones; Fc treatment: 35.07 \pm 13.08, n = 4; ephrin-A1 treated for 5 minutes: 15.97 \pm 1.62, n = 11; ephrin-A1 treated for 15 minutes: 8.38 \pm 1.58, n = 5; * P < 0.05 and ns = not significant by t-test).

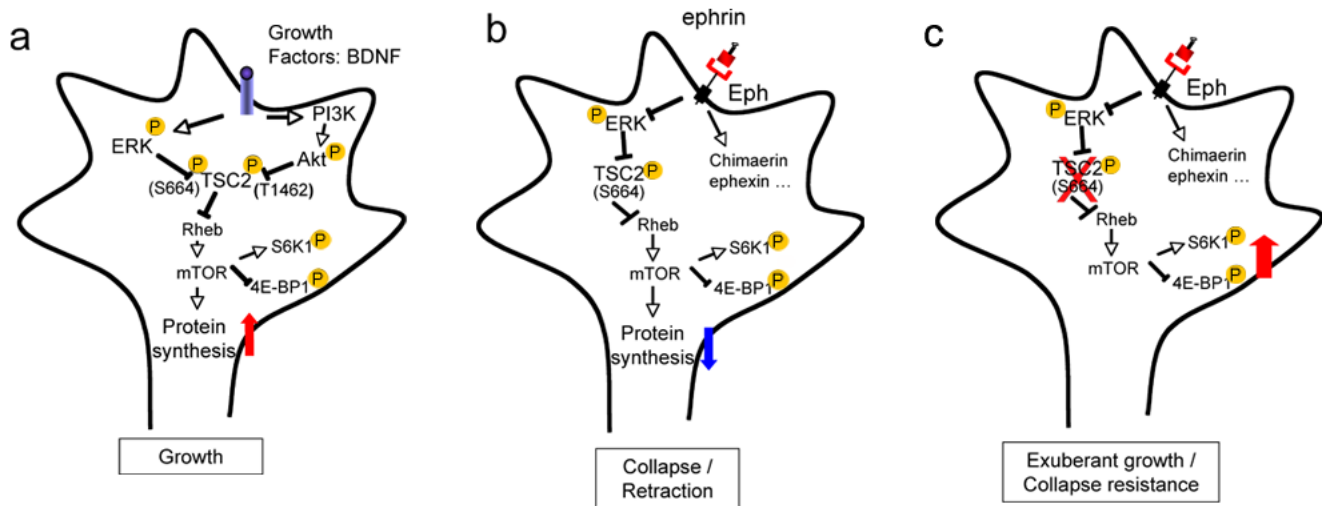


Figure S12. Proposed pathways used by ephrin and BDNF to regulate Tsc2 activity in axonal growth cone.

(a) Under growth promoting conditions, growth factors such as the neurotrophic factor BDNF activates both PI3-K/Akt and ERK pathways, which phosphorylate Tsc2 at Thr1462 and Ser664 sites, respectively. Tsc2 phosphorylation at these sites leads to increased protein synthesis and axonal growth/elongation via mTOR activation. (b) When an Eph-expressing growth cone comes into contact with ephrin ligands, Ephrin-Eph interaction causes inactivation of ERK and subsequent dephosphorylation of Tsc2 at Ser664. This results in suppression of mTOR activity and local protein synthesis, which contributes with growth cone retraction/collapse in concert with activation of other pathways involving Rho GTPase family modulating molecules such as ephexin and chimaerin. (c) In Tsc2 deficient neurons, mTOR is persistently activated leading to exuberant neurite growth, and rendering axons insensitive to the repulsive ephrin guidance signals. “→” indicates activation, and “--|” indicates inactivation.

Fig. 4c

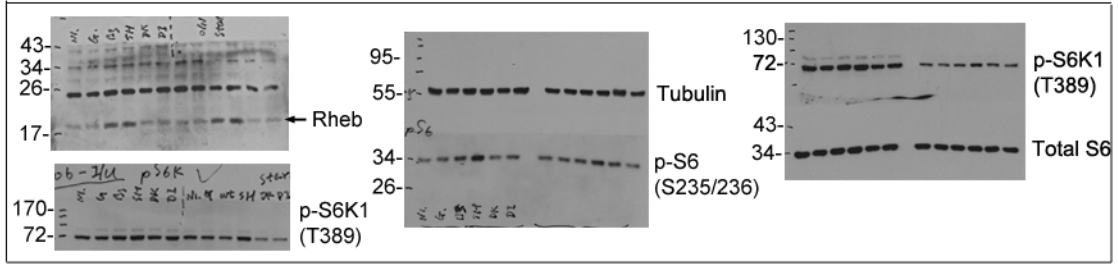


Fig. 5a

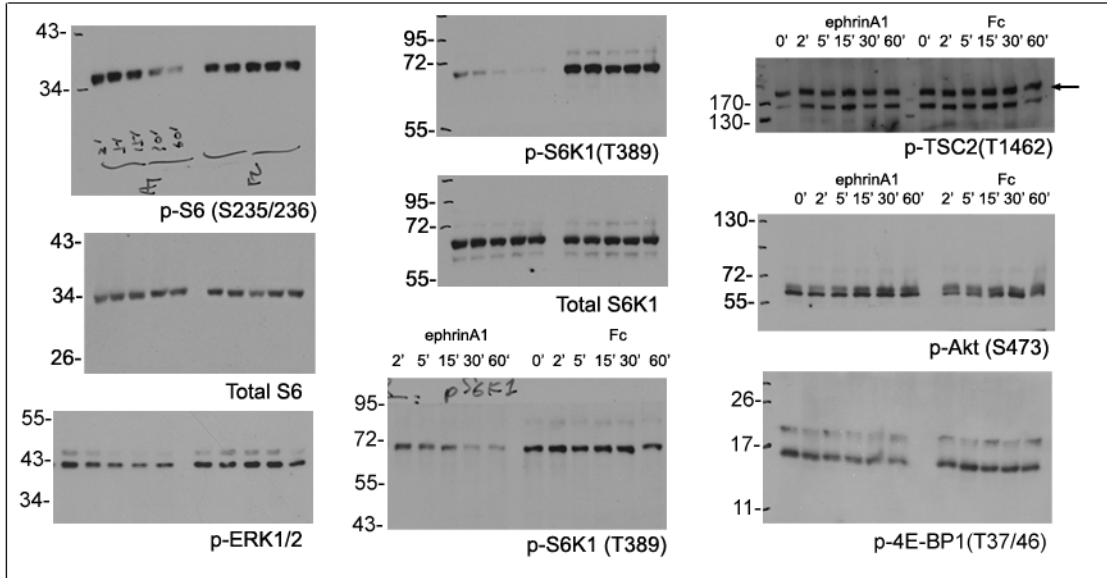


Fig. 5c

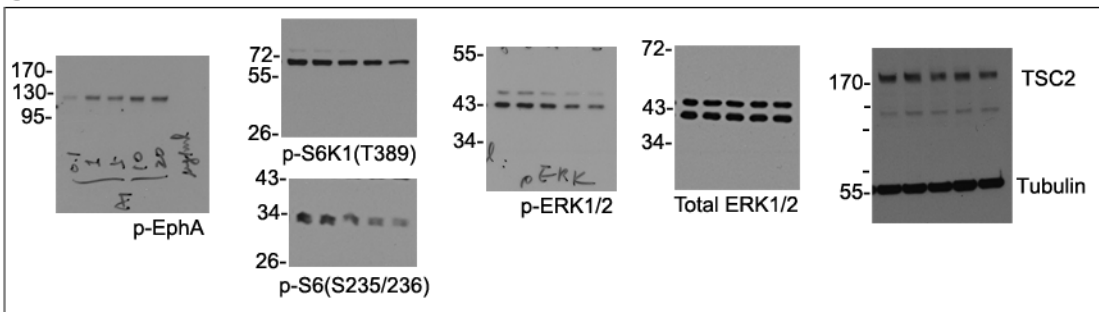


Fig. 5d

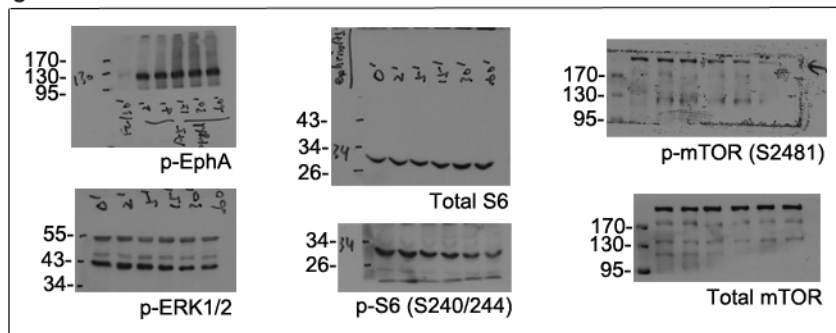


Figure S13. Full-length western blots for Figs. 4c, 5a, 5c and 5d .

Fig. 7a

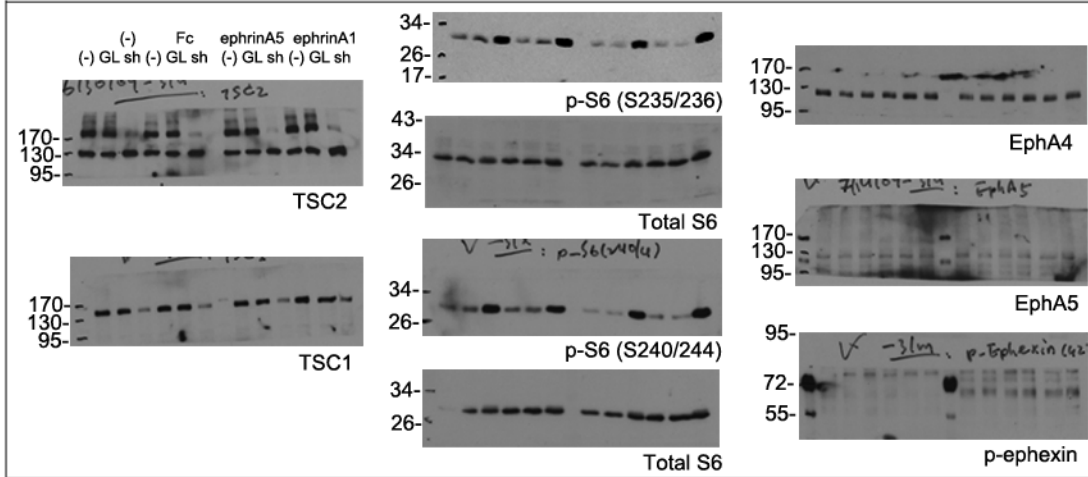
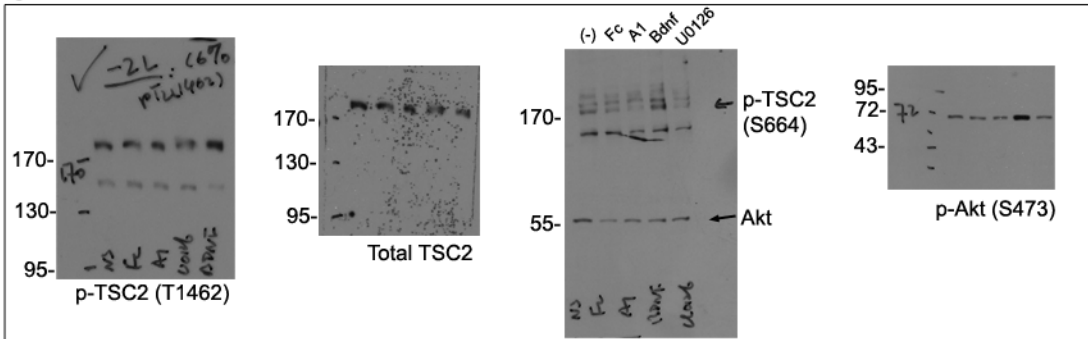
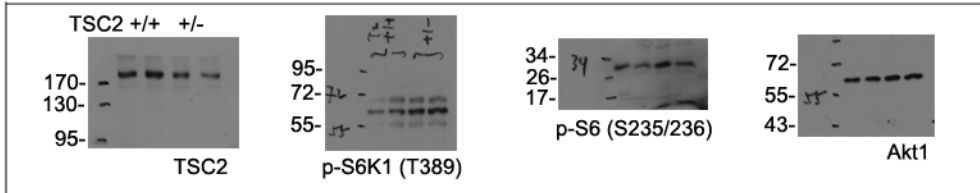


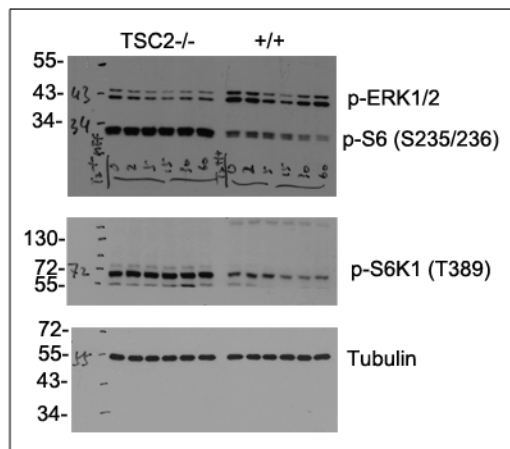
Fig. 8a



S4d



S10a



S10b

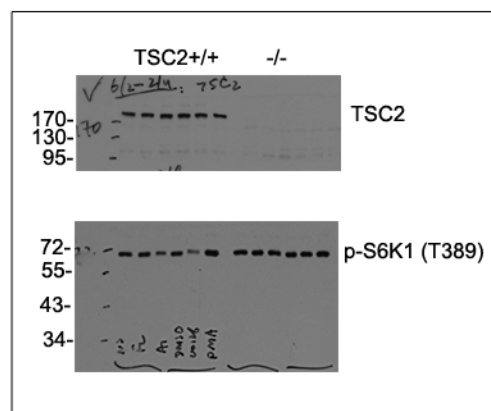


Figure S14. Full-length western blots for Figs. 7a, 8a, S4d, S10a and S10b.